RSC Advances

Volume 1 | Number 1 | Jan 2013 | Pages 1–100

RSC Advances

www.rsc.org/advances

ROYAL SOCIETY OF CHEMISTRY

ROYAL SOCIETY OF CHEMISTRY

www.rsc.org/advances

Naphtho[1,2‑b;5,6‑*b*’]difuran-based Donor-Accepter Polymers for High Performance Organic Field-Effect Transistors

Shaowei Shi,[1,2] *keli Shi,*[1,3] *Gui Yu,*[3]* *Xiaoyu Li,*[1,2]* *Haiqiao Wang*[1,2]*

1. State Key Laboratory of Organic-Inorganic Composites, Beijing University of Chemical Technology, Beijing 100029, China

2. Beijing Engineering Research Center for the Synthesis and Applications of Waterborne Polymers, Beijing University of Chemical Technology, Beijing 100029, China

3. Beijing National Laboratory for Molecular Sciences, Institute of Chemistry, Chinese Academy of Sciences, Beijing 100190, China

* Corresponding authors: e-mail: wanghaiqiao@mail.buct.edu.cn (H. Wang); yugui@iccas.ac.cn (G. Yu); lixy@mail.buct.edu.cn (X. Li)

ABSTRACT. Two naphthodifuran-based donor-acceptor copolymers are presented. *Via* reasonable main-chain modification and side-chain engeering, remarkably dense π–π stacking spacings (<3.5 Å) as well as high “edge-on” orientations are observed. When fabricated as organic field-effect transistors, high hole mobilities exceeding 5 cm^2 V^{-1} s^{-1} are achieved at a moderate annealing temperature of 120 °C.

KEYWORDS. polymer semiconductors, organic thin-film transistors, naphthodifuran, side-chain engineering, molecular packing

Over the past decades, conjugated donor-accepter (D-A) polymers have been extensively explored for use in flexible and low-cost electronic devices such as polymer solar cells and organic field-effect transistors (FETs), owing to their solution processability and superior mechanical properties.[1, 2] Among the numerous building blocks for constructing high-performance *p*-type polymer FETs, diketopyrrolopyrrole (DPP)[3, 4] and isoindigo (IID)[5-7] are definitely two of the most successful and frequently investigated acceptor units. By incorporating with different donor material such as oligothiophene,[8-10] thienothiophene,[11, 12] or (*E*)-2-(2-(thiophen-2-yl)vinyl)thiophene,[13-15] FETs based on these polymers have exhibited exciting hole moblities exceeding 1 cm^2 V^{-1} s^{-1}, and some even higher than 10 cm^2 V^{-1} s^{-1}. To achieve a high carrier mobility, an increased degree of crystallinity and a highly developed edge-on orientation of the polymer chains are always essential, which could be reached *via* smart molecular design (typically main-chain modification and side-chain engineering), or device optimalization (typically thermal annealing).

Recently, our group reported two *p*-type polymer semiconductors based on angular-shaped naphtho[1,2-b;5,6-*b*']difuran (NDF3) and DPP.[16a] Through the modification of the backbone structure, a moderate hole mobility of 0.56 cm^2 V^{-1} s^{-1} was obtained in PNDF3-T-DPP-based FET device. In subsequent measurement of grazing incident X-ray scattering diffraction (GIXRD), PNDF3-T-DPP film shows a very small π-π spacing (in plane) of 3.52 Å (see Figure

S7, 2θ = 25.3°), which is comparable with or even lower than that of current reported high performance *p*-type polymers. Obviously, the incorporation of this highly aromatic NDF3 unit into the main chain can effectively improve the crystallite packing of resulted films. However, although high mobilities of 3.6 cm^2 V^{-1} s^{-1} have been reported in naphthodifuran (NDF)-based solution-processed single-crystal FETs, for NDF-based conjugated polymers, the charge carrier transport is still low (less than 1 cm^2 V^{-1} s^{-1}). [16b]

Herein, *via* simple side-chain engineering, we report an optimal structure named PNDF3DPP-C24 by replacing the 2-octyldodecyl groups with the longer 4-decyltetradecan groups. Besides the extension of the alkyl chains for further improving the solubility, the branching point is moved far away from the conjugated backbone with the intention to reduce the steric hindrance between chains as well as strengthen the intermolecular π-π interactions.[15, 17-20] Remarkably, such a small change results in significantly enhanced carrier mobilities by almost one order of magnitude, which is measured to be 5.31 cm^2 V^{-1} s^{-1} at a gentle annealing temperature of 120 ^{o}C. A noteworthy feature is that, even when not subjected to a heat treatment, FETs based on PNDF3DPP-C24 film yield a rarely high mobility of 2.02 cm^2 V^{-1} s^{-1}. Moreover, to further investigate effects of different acceptors on the device performance, another electron-deficient isoindigo unit (also functionalized with 4-decyltetradecan groups) is copolymerized with NDF3 to construct PNDF3IID-C24. This is the first FET example of IID-based D-A copolymers using NDF3 as the donor unit. As a result, a hole mobility of 1.87 cm^2 V^{-1} s^{-1} is achieved in as-cast PNDF3IID-C24 film. After PNDF3IID-C24 film is annealed at 120 ^{o}C, the mobility increases to 3.35 cm^2 V^{-1} s^{-1}. All the values are among the highest hole mobilities of polymer semiconductors reported to date, and interestingly, we notice that, for PNDF3DPP-C24 and PNDF3IID-C24, the π–π stacking distances are measured as short as 3.46 and 3.48 Å, which are probably among the shortest π–π stacking distances for currently reported *p*-type conjugated polymers.[21, 22]

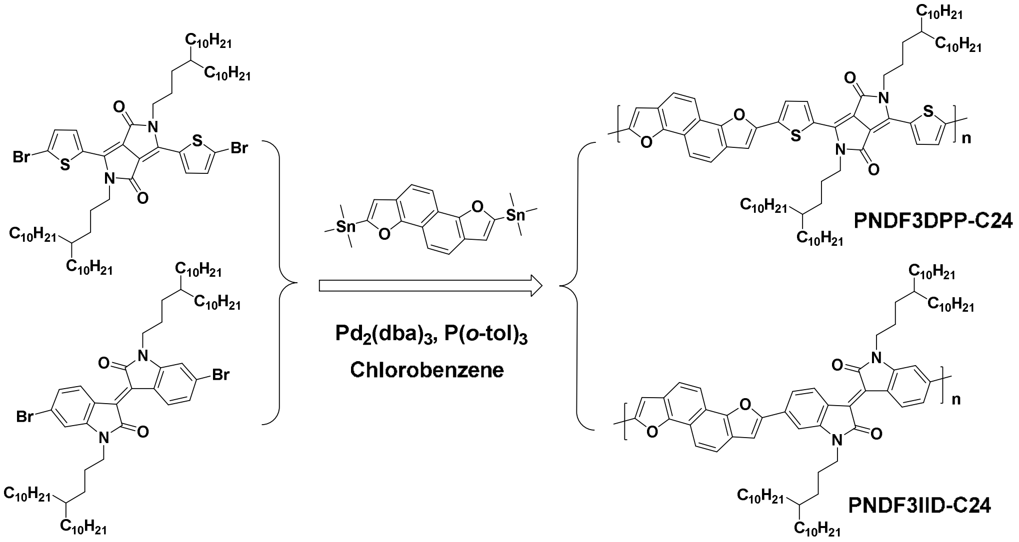

Figure 1. Synthesis and Chemical Structures of PNDF3DPP-C24 and PNDF3IID-C24

The detailed synthetic procedures and the characterization data of PNDF3DPP-C24 and PNDF3IID-C24 are presented in the Supporting Information (SI). Stille-coupling polymerization was employed in anhydrous chlorobenzene at 110 ^{o}C to afford the corresponding copolymers in high yields, followed with the purification by sequential Soxhlet extraction with methanol, acetone, and hexane to remove the oligomers and other impurities. Gel-permeation chromatography (GPC) at 150 °C with 1,2,4-trichlorobenzene as the eluent reveals number-averaged molecular weights (*M*n) of 66.6 and 31.2 kDa for PNDF3DPP-C24 and PNDF3IID-C24, with polydispersities (PDI) of 3.85 and 2.86 respectively. Both polymers can be readily soluble in hot chlorinated benzenes, and demonstrate excellent film-forming property. Highly uniform films can be easily fabricated using a simple spin-coating technique. Also, for PNDF3DPP-C24, it was found that a gelatin texture formed when a hot solution (~80 °C) was cooled to room temperature, even with a low concentration (5 mg/ml in *o*-dichlorobenzene) (See inserted picture in Figure 2a).

The absorption spectra of the two copolymers both in solution (chloroform) and in solid state (thin film) display similar features with a broad absorption band at long wavelength region (500-1000 nm for PNDF3DPP-C24, 400-750 nm for PNDF3IID-C24) (see Figure 2a and 2b), which is attributed to the intramolecular charge transfer (ICT) arising from strong donor–acceptor interactions. The bandgaps of PNDF3DPP-C24 and PNDF3IID-C24 in thin films calculated from the absorption onset are 1.49 and 1.70 eV, respectively. Note that the corresponding PNDF3IID-C24 thin-film absorption shows a slight blue-shift relative to its solution spectrum. This phenomenon has been reported with other IID- or DPP-based polymers, which may originate from the unique H-aggregation-induced interchain packing in the solid state.[18, 23] Cyclic voltammetry (CV) was performed to evaluate the molecular orbital energy levels of the polymers. The HOMO and LUMO energy levels as well as electrochemical bandgaps (E_g^{ec}) for PNDF3DPP-C24 and PNDF3IID-C24 are estimated as -5.25/-3.51/1.74 and -5.46/-3.47/1.99 eV, respectively. The electrochemically determined bandgaps are slightly higher (0.25~0.29 eV) than those on the basis of absorption edges data but can be accepted within the experimental error.

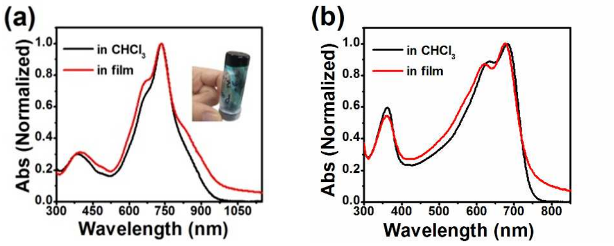

Figure 2. UV–vis absorption spectra of (a) PNDF3DPP-C24 and (b) PNDF3IID-C24. Inset in (a) is the picture of PNDF3DPP-C24 solution in *o*-dichlorobenzene (5 mg/ml) at room temperature.

To study the charge transport behavior of the polymers, bottom-gate/bottom-contact (BGBC) FETs were fabricated by spin-coating the polymer solutions in *o*-dichlorobenzene (7 mg/mL for PNDF3DPP-C24, 5 mg/ml for PNDF3IID-C24) on conventional octadecyltrichlorosilane (OTS)-modified Si/SiO_2 (300 nm) substrates. FET device characteristics were measured under ambient conditions. Typical transfer and output curves for PNDF3DPP-C24 and PNDF3IID-C24 based devices are shown in Figure 3. Surprisingly, the as-cast, spin-coated PNDF3DPP-C24 and PNDF3IID-C24 films show very high hole mobilities of 2.02 and 1.87 cm^2 V^{-1} s^{-1}, respectively, which are very rare among the currently reported *p*-type polymers.[15] For PNDF3DPP-C24, when the film is annealed at 80 ^{o}C, the mobility increases to 4.79 cm^2 V^{-1} s^{-1} and rises further to 5.31 cm^2 V^{-1} s^{-1} upon annealing at 120 ^{o}C for 5 min in air. Compared with previously reported PNDF3-T-DPP, which exhibits mobilities of 0.24 and 0.56 cm^2 V^{-1} s^{-1} at room and optimal annealing temperature, respectively, PNDF3DPP-C24 shows higher mobilities by almost one order of magnitude. For PNDF3IID-C24, similar growth trend of mobilities is observed, yielding a maximum mobility of 3.35 cm^2 V^{-1} s^{-1} after annealing at 120 ^{o}C, which is almost equal to the highest reported hole mobility (3.62 cm^2 V^{-1} s^{-1}) for IID-based polymers.[18]

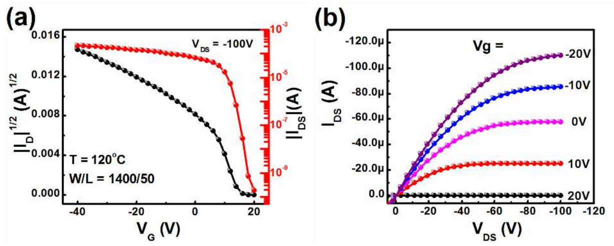

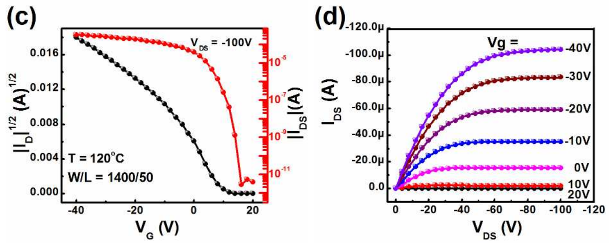

Figure 3. Transfer (left) and output (right) characteristics of the spin-coated film of polymer transistors based on OTS-modified Si/SiO$_2$ substrate: (a, b) PNDF3DPP-C24 with annealing at 120°C for 5 min; (c, d) PNDF3IID-C24 with annealing at 120°C for 5 min

Table 1. Optimized Electrical Parameters of Field-Effect Transistors

polymer	Annealing Temperature/°C	μ_h （cm^2 V^{-1} s^{-1}）	I_{on}/I_{off}	V_{th} （V ）
PNDF3DPP-C24	R.T.	2.02	10^6-10^7	15.2
	80	4.79	10^6-10^7	15.3
	120	5.31	10^6-10^7	14.6
PNDF3IID-C24	R.T.	1.87	10^7-10^8	10.3
	80	2.38	10^6-10^7	15.7
	120	3.35	10^7-10^8	8.6

Grazing incidence X-ray diffraction (GIXRD) was employed to deeply investigate the crystallinities and molecular orientations of the polymer thin films. As shown in Figure 4a and 4b, for as-cast PNDF3DPP-C24 and PNDF3IID-C24 thin films, the (*h*00) peaks (out-of-plane) up to the third orders are observed, indicating that highly ordered lamellar structures have formed even in the absence of thermal annealing. Upon thermal annealing at 120°C, diffraction patterns with increased intensity appear, demonstrating calculated lamellar *d*-spacings of 22.63

(PNDF3DPP-C24, 2θ = 3.9°) and 23.85 Å (for PNDF3IID-C24, 2θ = 3.7°), respectively. In the in-plane GIXRD spectra (Figure 4c and 4d), both PNDF3DPP-C24 and PNDF3IID-C24 demonstrate distinct diffraction peaks (010) at 2θ = 25.7 and 25.6°, corresponding to remarkably dense π−π stacking distances of 3.46 and 3.48 Å. To the best of our knowledge, both values are among the smallest either for DPP- or IID-based polymer semiconductors reported so far. Such narrow π−π spacing is preferable since it can reduce the energy barrier for interchain charge hopping, which is an important charge transport mechanism in polymer FETs, and thus, may contribute greatly to the high hole mobilities.[24] On the other hand, no clear (*h*00) peaks are observed in the in-plane patterns, indicating the formation of a predominant edge-on orientation respective to the substrates, which is also a major factor in generating the high FET performance because of the intermolecular interactions parallel to the direction of the channel current flow.[13]

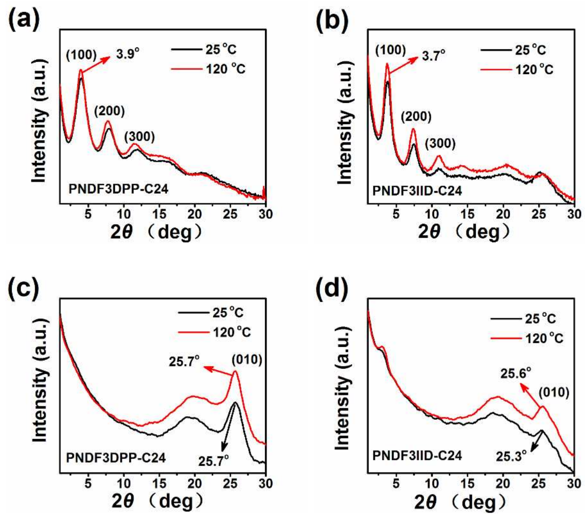

Figure 4. 1D-out-of-plane (a, b) and in-plane (c, d) GIXRD patterns of the polymer thin films.

Two-dimensional GIXRD (2D-GIXRD) was also performed to compare the ordering structure between PNDF3DPP-C24 and PNDF3IID-C24 (Figure 5a and 5b). Along the out-of-plane Q_z

axis, both the polymer films exhibit multiple diffraction peaks of the lamellar stacking repeat. For PNDF3DPP-C24, the reflection corresponding to π-stacking planes is clear along the in-plane Q_{xy} axis, showing that the orientation of these planes is largely perpendicular to the substrate. Furthermore, diffraction halos in the range of 4–5 Å are also observed, implying the occurrence of close interactions between the alkyl chains. [18] In contrast, PNDF3IID-C24 displays relatively weak (010) diffractions and diffraction halos, which is corresponding to the results of the 1D- in-plane GIXRD. From the atomic force microscopy (AFM) height image of each polymer film, it is observed that both polymer films exhibit highly fibrous interconnected networks with obviously crystallized zones, like other high-performance polymer FET materials containing DPP or IID unit. Such crystalline networks, which are likely the result of the strong intermolecular interactions, would form highly efficient pathways for charge carrier transport throughout the polymer film.

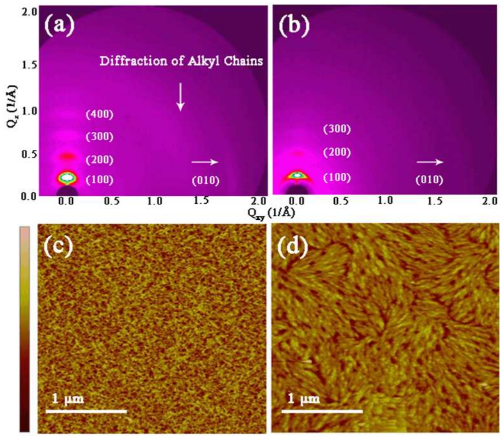

Figure 5. 2D-GIXRD patterns of (a) PNDF3DPP-C24 and (b) PNDF3IID-C24 after thermal annealing (120 °C). AFM height images (3×3 μm^2) of (c) PNDF3DPP-C24 and (d) PNDF3IID-C24 thin films on OTS-modified SiO_2/Si substrates with annealing at 120 °C

In conclusion, two NDF3-based D-A copolymers namely PNDF3DPP-C24 and PNDF3IID-C24, were synthesized and characterized. *Via* reasonable main-chain modification and side-chain engeering, remarkably small π−π stacking spacings of 3.46 and 3.48 Å are measured for PNDF3DPP-C24 and PNDF3IID-C24, respectively. GIXRD results display high edge-on orientations and well-ordered lamellar structures either in the as-cast or thermally annealed thin films. As a result, FETs based on PNDF3DPP-C24 and PNDF3IID-C24 films exhibit high hole mobilities of 2.02 and 1.87 $cm^2 V^{-1} s^{-1}$ even without a heat treatment. After annealing at 120 °C, increased hole mobilities up to 5.31 and 3.35 $cm^2 V^{-1} s^{-1}$ are achieved due to the enhanced crystalline tendency and intermolecular interaction, indicating the great potential of further structure/ device optimization based on these two skeletons.

AUTHOR INFORMATION

Corresponding Authors

wanghaiqiao@mail.buct.edu.cn (H. Wang); yugui@iccas.ac.cn (G. Yu); lixy@mail.buct.edu.cn (X. Li)

Author Contributions

S. Shi and K. Shi contributed equally to this work.

ACKNOWLEDGMENT

The GIXRD data were obtained at 1W1A, Beijing Synchrotron Radiation Facility. The authors gratefully acknowledge the assistance of the scientists of the Diffuse X-ray Scattering Station during the experiments. This work was financially supported by the Beijing Natural Science Foundation (2122047), the Specialized Research Fund for the Doctoral Program of Higher

Education (20130010110006), the National Science Foundation of China (51233006), the Major State Basic Research Development Program (2011CB808403), and the Strategic Priority Research Program of the Chinese Academy of Sciences (XDB 12030100).

REFERENCES

(1) Mei, J.; Diao, Y.; Appleton, A. L.; Fang, L.; Bao, Z. *J. Am. Chem. Soc.*, **2013**, *135*, 6724.

(2) (a) Li, Y. *Acc. Chem. Res.*, **2012**, *5*, 723. (b) Wu, W.; Liu Y.; Zhu, D. *Chem. Soc. Rev.*, **2010**, *39*, 1489.

(3) Li, Y.; Sonar, P.; Murphy, L.; Hong, W. *Energy. Environ. Sci*. **2013**, *6*, 1684.

(4) Nielsen, C. B.; Turbiez, M.; McCulloch, I. *Adv. Mater*., **2013**, *25*, 1859.

(5) Glowacki, E. D.; Voss, G.; Sariciftci, N. S. *Adv. Mater*., **2013**, *25*, 6783.

(6) Stalder, R.; Mei, J.; Graham, K. R.; Estrada, L. A.; Reynolds, J. R. *Chem. Mater.*, **2014**, *26*, 664.

(7) (a) Wang, E.; Mammo, W.; Andersson, M. R. *Adv. Mater*., **2014**, *26*, 1801. (b) Lei, T.; Wang, J.; Pei J. *Acc. Chem. Res.*, **2014**, *47*, 1117

(8) Yi, Z.; Sun, X.; Zhao, Y.; Guo, Y.; Chen, X.; Qin, J.; Yu, G.; Liu, Y. *Chem. Mater*., **2012**, *24*, 4350.

(9) Ha, J. S.; Kim, K. H.; Choi, D. H. *J. Am. Chem. Soc*., **2011**, *133*, 10364.

(10) Yi, Z.; Ma, L.; Chen, B.; Chen, D.; Chen, X.; Qin, J.; Zhan, X.; Liu, Y.; Ong, W. J.; Li, J. *Chem. Mater*., **2013**, *25*, 4290.

(11) Li, Y.; Singh, S. P.; Sonar, P. *Adv. Mater*., **2010**, *22*, 4862.

(12) Li, J.; Zhao, Y.; Tan, H. S.; Guo, Y.; Di, C.-A.; Yu, G.; Liu, Y.; Lin, M.; Lim, S. H.; Zhou, Y.; Su, H.; Ong, B. S. *Sci. Rep.*, **2012**, *2*, 754.

(13) Chen, H.; Guo, Y.; Yu, G.; Zhao, Y.; Zhang, J.; Gao, D.; Liu, H.; Liu, Y. *Adv. Mater.*, **2012**, *24*, 4618.

(14) Kang, I.; An, T. K.; Hong, J.-a.; Yun, H.-J.; Kim, R.; Chung, D. S.; Park, C. E.; Kim, Y.-H.; Kwon, S.-K. *Adv. Mater.*, **2013**, *25*, 524.

(15) Kang, I.; Yun, H.-J.; Chung, D. S.; Kwon, S.-K.; Kim, Y.-H. *J. Am. Chem. Soc.*, **2013**, *135*, 14896.

(16) (a) Shi, S.; Xie, X.; Gao, C.; Shi, K.; Chen, S.; Yu, G.; Guo, L.; Li, X.; Wang, H. *Macromolecules*, **2014**, *47*, 616. (b) Mitsui, C.; Soeda, J.; Miwa, K.; Tsuji, H.; Takeya, J.; Nakamura, E. *J. Am. Chem. Soc.*, **2012**, *134*, 5448. (c) Nakano, M.; Mori, H.; Shinamura, S.; Takimiya, K. *Chem. Mater.*, **2012**, *24*, 190. (d) Liu, B.; Chen, X.; He, Y.; Xiao, L.; Li, Y.; Zhou, K.; Fan, L.; Zou, Y. *RSC Adv.*, **2013**, *3*, 5366.

(17) Mei, J.; Kim do, H.; Ayzner, A. L.; Toney, M. F.; Bao, Z. *J. Am. Chem. Soc.*, **2011**, *133*, 20130.

(18) Lei, T.; Dou, J. H.; Pei, J. *Adv. Mater.*, **2012**, *24*, 6457.

(19) Lee, J.; Han, A. R.; Kim, J.; Kim, Y.; Oh, J. H.; Yang, C. *J. Am. Chem. Soc.*, **2012**, *134*, 20713.

(20) Lee, J.; Han, A. R.; Yu, H.; Shin, T. J.; Yang, C.; Oh, J. H. *J. Am. Chem. Soc.*, **2013**, *135*, 9540.

(21) Fan, J.; Yuen, J. D.; Cui, W.; Seifter, J.; Mohebbi, A. R.; Wang, M.; Zhou, H.; Heeger, A.; Wudl, F. *Adv. Mater.*, **2012**, *24*, 6164.

(22) Osaka, I.; Shimawaki, M.; Mori, H.; Doi, I.; Miyazaki, E.; Koganezawa, T.; Takimiya, K. *J. Am. Chem. Soc.*, **2012**, *134*, 3498.

(23) Shin, J.; Um, H. A.; Lee, D. H.; Lee, T. W.; Cho, M. J.; Choi, D. H. *Poly. Chem.*, **2013**, *4*, 5688.

(24) Chen, M. S.; Lee, O. P.; Niskala, J. R.; Yiu, A. T.; Tassone, C. J.; Schmidt, K.; Beaujuge, P. M.; Onishi, S. S.; Toney, M. F.; Zettl, A.; Fréchet, J. M. J. *J. Am. Chem. Soc.*, **2013**, *135*, 19229.

Insert Table of Contents Graphic